Bridging Simulations and Experiments in Microstructure Evolution

M. C. Demirel,[1,2,3] A. P. Kuprat,[2] D. C. George,[2] and A. D. Rollett[3]

[1]*Materials Science and Technology, MST-8, Los Alamos National Laboratory, Los Alamos, New Mexico 87545*
[2]*Theoretical Division, T-1, Los Alamos National Laboratory, Los Alamos, New Mexico 87545*
[3]*Carnegie Mellon University, Department of Materials Science & Engineering, Pittsburgh, Pennsylvania 15213*

(Received 28 May 2002; published 9 January 2003)

We demonstrate the importance of anisotropic interface properties in microstructure evolution by comparing computed evolved microstructures to final experimental microstructures of 5170 grains in 19 thin aluminum foil samples. This is the first time that a direct experimental validation of simulation has been performed at the level of individual grains. We observe that simulated microstructures using curvature-driven grain boundary motion and anisotropic interface properties agree well with experimentally evolved microstructures, whereas agreement is poor when isotropic properties are used.

DOI: 10.1103/PhysRevLett.90.016106 PACS numbers: 68.35.–p, 68.37.Hk, 68.55.Jk, 81.40.–z

This paper seeks to extend previous statistical comparisons of predicted and experimentally observed grain boundary network evolution by demonstrating agreement at the scale of individual grains, provided that the anisotropy of interfacial energy and mobility is included. With very few exceptions [1], only statistical comparisons have been made such as determining the exponent in the power-law relationship between average radius and time. In addition to this general aim, we consider coarsening in networks of low angle grain boundaries (subgrains), which has been the subject of some controversy. Some authors have postulated that the interfaces are essentially sessile because they are themselves networks of lattice dislocations and that coarsening occurs by rotation of individual subgrains [2,3]. Rotation is driven by minimization of interfacial energy and tends to eliminate the misorientation between certain pairs of adjacent grains, thus causing coalescence and coarsening to occur. Gleiter, on the other hand, showed that low angle grain boundaries migrate under curvature driving forces just as observed for high angle grain boundaries [4]. Clearly, both mechanisms are feasible for coarsening of subgrain networks, and so it is of some importance to determine which one is applicable to real materials. Since the torque that drives grain rotation is supralinear in (inverse) grain size, it is reasonable to expect that curvature-driven migration dominates at the large grain sizes observed in this experiment whereas rotation should dominate in nanoscale grain sizes.

We have previously shown a strong agreement between small-scale grain growth experiments and anisotropic three-dimensional simulations [5] obtained from electron backscatter diffraction (EBSD) measurements [6]. Using the same technique, we obtained data for 5170 grains from 19 thin aluminum foil samples with columnar grain structure (thereby avoiding serial sectioning) and compared our computational results with experiments.

Our simulation model uses curvature-driven motion implemented by GRAIN3D [7], a three-dimensional, gradient-weighted moving finite elements code. We assume that the grain boundary motion is proportional to the local mean curvature of the interface,

$$v_n = \mu\sigma\kappa, \tag{1}$$

where v_n is the normal velocity of the interface, μ is the grain boundary mobility, and σ is the interface energy per unit area. κ is the sum of principal curvatures, i.e., twice the mean curvature; in these simulations, the curvature is equal to the curvature observed in the plane. The interfaces are represented as piecewise linear. For details of the simulation method, the reader should refer to Ref. [7].

The interfacial anisotropy is based on a previous determination of grain boundary energy, σ, and mobility, μ, from a statistical/multiscale analysis of triple junction geometry and crystallography in aluminum [8–10], and the result for energy is in very good agreement with the Read-Shockley model [11] as expected. In the highly textured, columnar grain structure aluminum foil we investigated, most interfaces are low angle boundaries (misorientation $<15°$). The grain boundary mobility is low for small misorientations but undergoes a sharp transition to high mobilities between 10° and 15° in misorientation which is in agreement with the literature [12–14]. For our simulations, we assume that all high angle grain boundaries ($> 15°$) have the same values of energy and mobility. The occurrence of high angle boundaries is very low in this material, which means that only a small error is introduced by this assumption. This experiment permitted a verification of curvature-driven interface motion [4], as compared with the competing mechanism of grain rotation [3] leading to coalescence [2]. We found a standard deviation of 0.98° in misorientation angle between the initial and final experimental

states, implying insignificant rotation of the boundary [15] and that interface motion is indeed curvature driven.

To generate input for the simulation from EBSD experimental results, grain boundaries and triple junctions are located from the recorded image, and the grain boundary structure on the section plane is extruded to create the three-dimensional mesh [16,17]. We use the EBSD measurements to assign a single average orientation for each grain and thus a single interface misorientation for each pair of grains. Using the results of Yang *et al.*, the interface misorientation gives a relative value of σ and μ for each interface. Note that use of a constant value of σ along the boundary from one triple junction to the other means that our model does not include boundary inclination dependence. The total volume of the structure is kept constant and exterior boundaries are assumed to be quasiperiodic [5]. Figure 1(A) shows a representative experimental input. The simulation was initialized with this state and was run until the area match function, explained in the next paragraph, began to decrease. The final experimental microstructure is shown in Fig. 1(B), and is to be compared to the computed evolved microstructure shown in Figs. 1(C) and 1(D). A strong cube texture, $\{100\}\langle 001\rangle$, was observed for both the initial and the final experimental microstructures. This is as expected because of the small amount of coarsening that has taken place during the experiment.

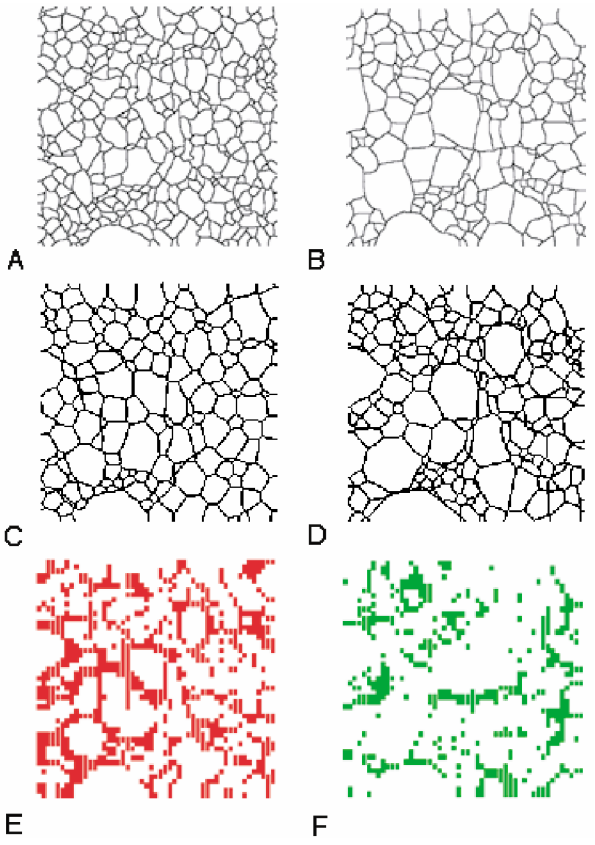

FIG. 1 (color online). (A) Initial experimental microstructure (top view) with dimensions 2000 μm $\times$ 2000 μm (339 grains). (B) Final experimental microstructure. (C) Isotropic mobility simulation final state. (D) Anisotropic mobility simulation final state. (E) Pixelized subtractions of (C) from (B). (F) Pixelized subtraction of (D) from (B).

Simulations were performed with three different assumptions for the interface properties. First, μ and σ were assumed constant and equal to unity (isotropic). Second, μ was allowed to depend on the misorientation angle (anisotropic mobility). Third, μ and σ were allowed to depend on the misorientation angle (anisotropic mobility and energy). For quantitative comparison, we introduce a regular grid of sampling points $s(x, y)$ of between 2500 and 10 000 points depending on the size of the microstructure. A quantitative measure for the comparison is then given by a normalized area match function (NAMF). One may think of this comparison method as overlaying the final experimental state onto successive simulation snapshots and measuring at each snapshot time the amount of area where the orientations match. The higher the value, the better the match.

$$\mathrm{NAMF}_i = \frac{1}{Z}\sum_{x,y} \delta[s_i(x, y) - s_{\mathrm{exp}}(x, y)], \qquad (2)$$

where for simulation snapshot i, s_i is the crystal orientation, and s_{exp} is the crystal orientation for the final experimental configuration, δ is the delta function, and Z is the number of sampling points. If the crystal orientation for the spatial point (x, y) is the same as the final experimental crystal orientation at the same location, the delta function is one, otherwise it is zero. NAMF_i is then given by summing over the set of all (x, y) points and dividing by the total number of points. Perfect agreement is denoted by NAMF $= 1$ and perfect disagreement by NAMF $= 0$. Since the final experimental state evolved from the initial experimental state, which is identical to the initial simulation state, the comparison begins with a high degree of match. In a representative microstructure, we find a 62% match between the initial simulation state and the final experimental state (NAMF $= 0.62$). Figure 2(A) shows the results of isotropic and anisotropic simulations for one sample. In the isotropic case, the maximum NAMF gives a 68% match, whereas both anisotropic cases reach a significantly higher maximum NAMF. Figures 1(E) and 1(F) illustrate the pixelized comparison of experimental to simulated final states from which NAMF is calculated. All simulations eventually exhibit a decreased match as they were run longer than the equivalent final experimental time. It is clear from these results that anisotropic interface properties play an important part in microstructure evolution. With regard to simulations involving anisotropic energy, we observed violations of the wetting condition (Young's equation) at some triple junctions. These force imbalances occur at triple junctions where one of the three energies is

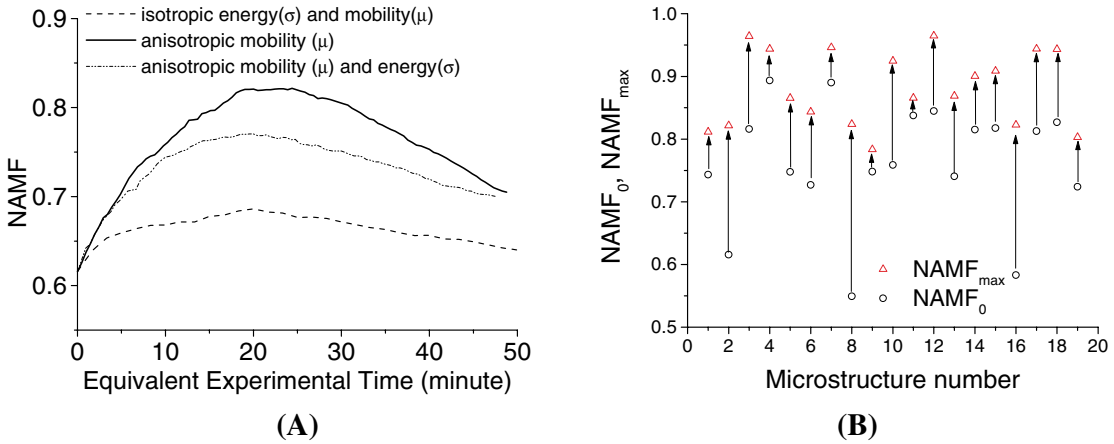

FIG. 2 (color online). (A) Results of a representative simulation with different interface properties: The isotropic case reaches a maximum NAMF value of 0.68, accounting for 16% of the match; both anisotropic cases reach maximum NAMF values between 0.82 and 0.77, accounting for 53% and 40% of the match, respectively. (B) $NAMF_{max}$ and $NAMF_0$ values for 19 microstructures.

greater than the sum of the other two and can result from using a constant σ along the entire interface. To prevent this, we constrained the dihedral angles so that they are always larger than 90° by adding an isotropic minimum energy to all boundaries [15]. Because of the uncertainty of the effects of adjusting σ in this manner, we consider only the anisotropic mobility simulations in the remainder of this Letter.

Scaling the 19 simulation times so that the average of all simulations matches the experimental time of 20 min at 550 °C, we find a low standard deviation, 1.80 min, suggesting that simulated evolution and experimental grain growth are consistent. In Fig. 2(B), for each of the 19 simulations using anisotropic mobility properties, we display a vector representing the amount of experimental microstructure evolution matched by the simulation. Each vector origin gives $NAMF_0$ or the amount of match between the final experimental state and the initial microstructure state. Each vector tip shows the $NAMF_{max}$ or the amount of match between the experimental and simulated final states. To compare the observed experimental microstructure evolution with the anisotropic simulated evolution, we calculate the mean (0.5) and standard deviation (0.172) of $(NAMF_{max} - NAMF_0)/(1 - NAMF_0)$, showing that our simulation model accounts for 50% of the microstructure evolution observed in experiment. The mean and standard deviation for isotropic simulations are 0.17 and 0.147, respectively.

The comparison between the experiment and computation at the individual grain level extends our knowledge of grain evolution. First, microstructural evolution in columnar aluminum foils can be correctly modeled using anisotropic parameters. The results of three-dimensional computer simulations using anisotropic mobility agree well with experimental grain growth. Second, we have shown that isotropic modeling has very little predictive value. Using NAMF as a metric, we have shown that isotropic modeling explains at most 17% of the evolution, whereas anisotropic modeling accounts for 50% of the evolution. The failure of our model to account for all the evolution may be due to one or more of the following: boundary inclination dependence, computational indeterminacy due to grain topology changes [7], dislocation density, stored deformation energy, or by sample error such as surface defects, sample preparation, local deformations, and grains that are not columnar. Additionally, in these mesoscale experiments, we observed a 0.98° standard deviation in misorientation angle between initial and final experimental states implying insignificant grain rotation and that microstructure evolution is curvature driven.

This research is support by Los Alamos National Laboratory (DOE, W-7405-ENG-36), the MRSEC program of NSF (DMR-0079996), and the Computational Materials Science Network (US-DOE).

[1] T. Baudin, P. Paillard, and R. Penelle, Scr. Mater. **40**, 1111 (1999).
[2] H. Hu, in *Recovery and Recrystallization of Metals*, edited by L. Himmel (Interscience, New York, 1963), p. 362.
[3] G. Martin, Phys. Status Solidi B **172**, 121 (1992).
[4] H. Gleiter, Philos. Mag. **20**, 821 (1969).
[5] M. C. Demirel *et al.*, Interface Sci. **10**, 137 (2002).
[6] M. C. Demirel *et al.*, in *Electron Backscatter Diffraction in Materials Science*, edited by M. K. Adam, J. Schwartz, and Brent L. Adams (Kluwer Academic, New York, 2000), p. 65.
[7] A. P. Kuprat, SIAM J. Sci. Comput. **22**, 535 (2000).
[8] B. L. Adams *et al.*, Scr. Mater. **38**, 531 (1998).

[9] D. Kinderlehrer *et al.*, in *Proceedings of the Twelfth International Conference on Textures of Materials* (NRC Research Press, Montréal, Canada, 1999), p. 1643.
[10] C.-C. Yang, W.W. Mullins, and A. D. Rollett, Scr. Mater. **44**, 2735 (2001).
[11] W.T. Read and W. Shockley, Phys. Rev. **78**, 275 (1950).
[12] R. Viswanathan and C. L. Bauer, Acta Metall. **21**, 1099 (1973).
[13] R. Sandstrom, Acta Metall. **25**, 897 (1977).
[14] D. A. Smith *et al.*, *Grain Boundary Structure and Kinetics* (American Society for Metals, Metals Park, Ohio, 1980).
[15] M. C. Demirel, in *Materials Science and Engineering* (Carnegie Mellon University, Pittsburgh, 2002), p. 127.
[16] B. R. Schlei, in SPIE Conference Proceedings, Seattle, 2002, Vol. XI (to be published).
[17] M. C. Demirel *et al.*, J. Appl. Phys. (to be published).